

# Spatiotemporal Co-attention Recurrent Neural Networks for Human-Skeleton Motion Prediction

Xiangbo Shu, Liyan Zhang, Guo-Jun Qi, Wei Liu, and Jinhui Tang

**Abstract**—Human motion prediction aims to generate future motions based on the observed human motions. Witnessing the success of Recurrent Neural Networks (RNN) in modeling the sequential data, recent works utilize RNN to model human-skeleton motion on the observed motion sequence and predict future human motions. However, these methods did not consider the existence of the spatial coherence among joints and the temporal evolution among skeletons, which reflects the crucial characteristics of human motion in spatiotemporal space. To this end, we propose a novel Skeleton-joint Co-attention Recurrent Neural Networks (SC-RNN) to capture the spatial coherence among joints, and the temporal evolution among skeletons simultaneously on a skeleton-joint co-attention feature map in spatiotemporal space. First, a skeleton-joint feature map is constructed as the representation of the observed motion sequence. Second, we design a new Skeleton-joint Co-Attention (SCA) mechanism to dynamically learn a skeleton-joint co-attention feature map of this skeleton-joint feature map, which can refine the useful observed motion information to predict one future motion. Third, a variant of GRU embedded with SCA collaboratively models the human-skeleton motion and human-joint motion in spatiotemporal space by regarding the skeleton-joint co-attention feature map as the motion context. Experimental results on human motion prediction demonstrate the proposed method outperforms the related methods.

**Index Terms**—Human Motion Prediction, Spatiotemporal Co-attention, Gated Recurrent Unit, Attention Mechanism, Recurrent Neural Network.

## 1 INTRODUCTION

WITH the development of the MOCAP devices<sup>1</sup>, such as Kinect, PS Move and Vicon, capturing human-skeleton motions becomes easy and convenient. At present, more and more MOCAP-based products are emerging in various application areas, such as somatic game, Virtual Reality (VR), and human-machine interactions, etc. One of the key technologies behind these products are the human-skeleton motion analysis. Human-skeleton motion analysis is an interesting topic in the computer vision area, generally including motion synthesis, motion prediction, pose estimation and so on [1], [2], [3], [4]. Besides, many researchers have also attempted to understand the human action, interaction and even activity in video by taking the human-skeleton motion as a crucial motion information [5], [6], [7], [8].

In this work, we focus on the human motion prediction task that aims to generate the future skeleton motions based on the observed skeleton motion sequence captured by the MOCAP. In the early stages, due to the sequentiality and nonlinearity of human motions, researchers utilized various probabilistic models, such as latent variable model [9], Markov model [3], [10], generative model [11], to predict human motion based on a number of observed human mo-

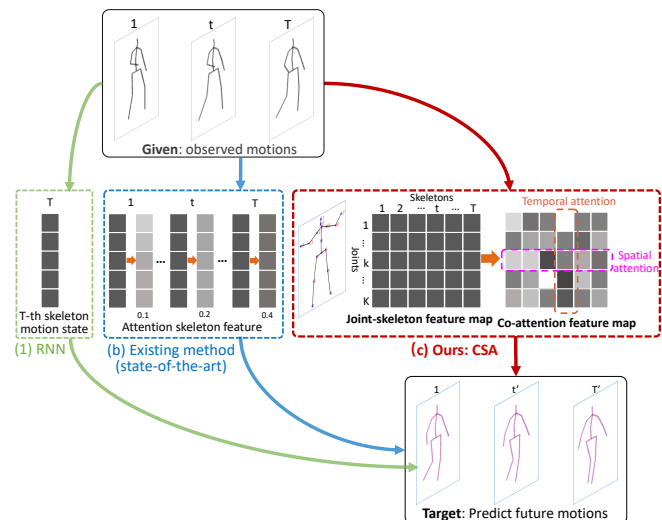


Fig. 1. Idea of Skeleton-joint Co-Attention (SCA). Existing methods only learn the skeleton-attention feature vectors in temporal space, where all elements in a vector are assigned with the same attention factor. Our SCA dynamically learns a skeleton-joint co-attention feature map of human joints and skeletons in spatiotemporal space, where all elements in such feature map are assigned with different attention factors. SCA will be embedded into a variant of RNN, called Spatiotemporal Co-Attention RNN (SC-RNN) in this paper.

X. Shu, and J. Tang are with the School of Computer Science and Engineering, Nanjing University of Science and Technology, Nanjing 210094, China. E-mail: {shuxb, jinhuitang}@njust.edu.cn.

L. Zhang is with the College of Computer Science and Technology, Nanjing University of Aeronautics and Astronautics, Nanjing 210016, China. E-mail: zhangliyan@nuaa.edu.cn.

G.-J. Qi is with the Huawei Cloud, Bellevue, WA 98004, USA. E-mail: guojun.qi@huawei.com.

W. Liu is with the Computer Vision Group, Tencent AI Lab, Shenzhen 518000, China. E-mail: wliu@ee.columbia.edu.

1. [https://en.wikipedia.org/wiki/Motion\\_capture](https://en.wikipedia.org/wiki/Motion_capture)

tions. Recently, Recurrent Neural Networks (RNN) [12], especially Gated Recurrent Unit (GRU) [13], and Long Short-Term Memory (LSTM) [14], has shown remarkable performance in capturing the sequential information compared with traditional methods [15], [16], [17]. Therefore, recent RNN-based methods [1], [18], [19] used RNN to model the

sequential motions over time for addressing the problem of human motion prediction.

In above RNN-based motion prediction methods, the direct propagation of motion information only happens between the consecutive frames. Although RNN can predict a satisfactory short-term motion, it weakly predicts one long-term motion only by the motion state updated in the previous frame [20]. To address this problem, a straightforward way is that we can directly propagate all the observed motions into one future frame for predicting the long-term motion in RNN. In other words, we can set all the observed motions as a new motion context, which directly propagates into one future frame in RNN. However, not all observed motions equally contribute to the prediction of one specific future motion. Therefore, Tang et al. [20] presented a temporal attention mechanism (namely skeleton attention) that dynamically learns an attention factor for each observed motion based on their contribution to the prediction of one future motion. In this work, by regarding all the observed motions as the motion context, we utilize RNN with skeleton-attention mechanism to predict future motion.

Moreover, most RNN-based motion prediction methods model human-skeleton motions only in temporal space, which ignore the spatial coherence among human joints in spatial space. For example, in the “walking” action, the swing directions of left(right) arm and right(left) leg are usually consistent with each other in spatial space. Some previous action recognition methods have validated that exploring the spatial dependence among joints and the temporal dependence among skeletons can further improve the performance on human action recognition [21], [22]. Therefore, we consider exploring the spatial coherence among human joints and temporal evolution among human skeletons simultaneously via an attention mechanism in spatiotemporal space (not a single space).

Motivated by this, we design a new **Skeleton-joint Co-Attention (SCA)** mechanism to well capture the whole human motion information by learning the skeleton-joint co-attention factors of all observed motions in spatiotemporal space, as shown in Figure 1. We firstly construct a skeleton-joint feature map to represent all the observed motions, in which one row and column indicate a joint-type feature and skeleton-type feature of human motion in the spatial and temporal spaces, respectively. On the skeleton-joint feature map, SCA dynamically learns the skeleton-attention factors of human skeletons in temporal space, and the joint-attention factors of human joints in spatial space. At each time step, we can obtain a skeleton-joint co-attention feature map, which refines the useful observed motion corresponding to one future motion by the different attention factors. As we know, in conventional attention models, one feature vector is assigned with an attention factor in a single space, e.g., temporal space. Unlike conventional attention models, in SCA, each element in the skeleton-joint co-attention feature map is assigned with a skeleton-joint co-attention factor (obtained through multiplying a skeleton-attention factor by a joint attention factor) in multiple spaces (i.e., both spatial and temporal spaces) that measures its contribution to the prediction of one future motion in spatiotemporal space.

Based on the designed SCA, we propose a novel

**Skeleton-joint Co-attention Recurrent Neural Networks (SC-RNN)** to simultaneously capture the spatial coherence among joints and the temporal evolution among skeletons on a co-attention feature map in spatiotemporal space. Figure 2 shows the training framework of SC-RNN. Specifically, SC-RNN models human-skeleton motions and human-joint motions simultaneously, by regarding the skeleton-joint co-attention feature map as a new motion context. And then, the predicted human-skeleton motions and human-joint motions are integrated to predict the future motion by a new spatial confidence gate at each time step. Finally, we propose a new weighted gram-matrix loss to measure the errors between the predicted motion and the ground-truth motion in the model learning. In this work, we conduct experiments on human motion prediction to show the superiority of the proposed SC-RNN compared with the related methods.

Over all, the main contributions of this work are summarized as follows:

- We propose a novel Skeleton-joint Co-attention Recurrent Neural Network (SC-RNN) to simultaneously capture the spatial coherence among joints and the temporal evolution among skeletons in spatiotemporal space.
- We design a new Skeleton-joint Co-Attention (SCA) mechanism to dynamically refine the observed motion information over time by learning a skeleton-joint co-attention feature map on the observed human motion sequence.
- To learn SC-RNN, we propose a new weighted gram-matrix loss that exploits the correlations between two skeletons, which ensures the predicted skeletons with high correlation having the similar location.

The rest of this paper is organized as follows. Section 2 reviews some works related to skeleton-based action recognition, and human-skeleton motion prediction. Section 3 introduces the proposed method in details. Experiments are conducted in Section 4, followed by the conclusions in Section 5.

## 2 RELATED WORK

In this section, we briefly review some works related to the skeleton-based action recognition and human-skeleton motion prediction.

### 2.1 Skeleton-based Action Recognition

Human action recognition is a long-standing research topic in computer vision and pattern recognition communities, which aims to enable a computer to automatically understand the action performed by people [23], [24], [25]. In the task of action recognition, the input data are RGB image or skeleton of each frame. Based on different input data, action recognition can be mainly categorized two classes, i.e., RGB-based action recognition and skeleton-based action recognition. In RGB-based action recognition, the input features are the visual features of RGB-image in each frame [15], [16], [26], [27], and sometimes they are attached the flow features [28], [29], [30], [31], [32]. In skeleton-based action recognition, the input features are the positions of the

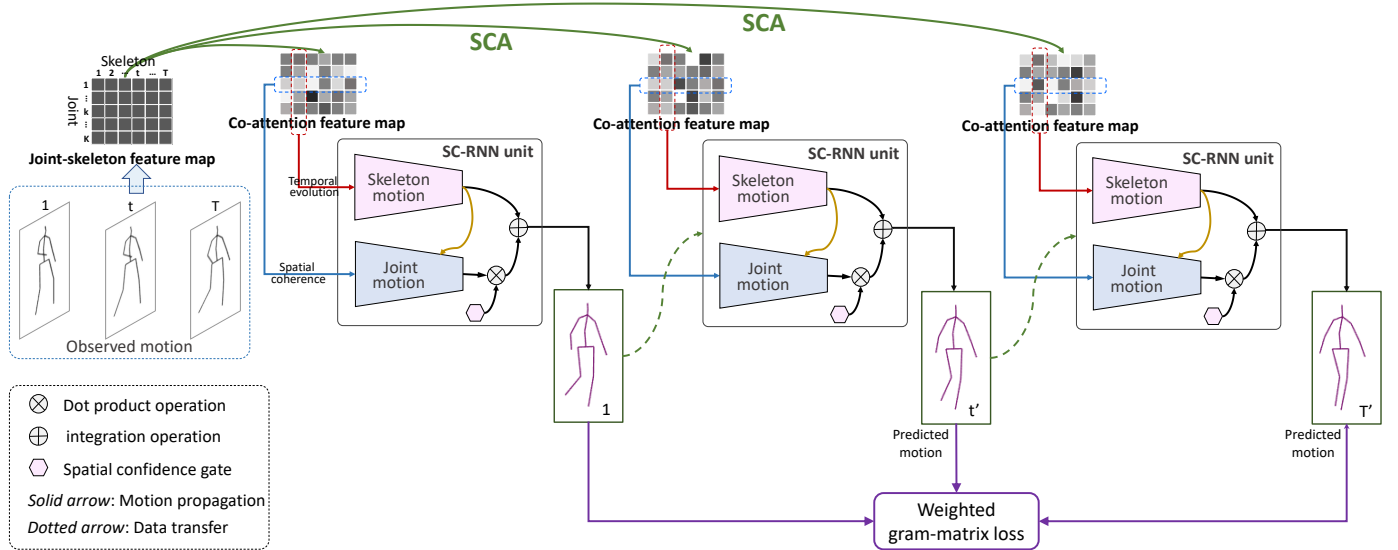


Fig. 2. Framework of the proposed SC-RNN in modeling human motions. At each time step, a co-attention feature map of all the observed motions is firstly learned by Skeleton-joint Co-Attention (SCA) in spatiotemporal space. CS-RNN models human-skeleton motions and human-joint motions in spatiotemporal space by regarding the skeleton-joint co-attention feature map as a new motion context. A new weighted gram-matrix loss is presented to learn SC-RNN in the training phase.

skeleton [21], [33], [34], [35], [36], [37]. We will mainly focus skeleton-based action recognition in this paper.

As one of the earliest works, Yacoob and Black [38] proposed to model the time-scale and time-shifted activity by Principal Component Analysis (PCA). Subsequently, some researchers proposed various models to learn representations of actions [34], [39], [40], [41], [42]. For example, since the tracked 3D positions of human joints may be wrong, Wang et al. [34] proposed an “actionlet” ensemble model to learn the representation of each action by capturing the intra-class variance. Shahroudy et al. [41] divided the human motion into several body parts, and proposed a joint sparse regression method to utilize the structured sparsity to model the features from a subset of the body parts.

Recently, Deep neural Network has been employed to learn the more discriminative representations of actions [37], [43], [44], [45]. In particular, as an advantage for handling sequential data with variable length [18], [46], Recurrent Neural Networks, including Gated Recurrent Unit, and Long Short-Term Memory (LSTM), has made impressive progress in skeleton-based action recognition [5], [6], [21], [22], [33], [35], [47], [48]. One of the most representative works is that Du et al. [6] divided a human body skeleton into five parts, and then fed these five parts into five RNNs. As the number of layers increases, the outputs of multiple RNNs are hierarchically fused, and input to the following RNNs. Besides, Liu et al. [22], [33] utilized LSTM to model the temporal and spatial dependencies among human motions for better understanding human action in the skeletal data. Likewise, Wang et al. [21] proposed a two-stream RNN (i.e., temporal RNN and spatial RNN) architecture to model temporal motions of skeletons over time and spatial relations among skeleton joints. These methods hold that all human joints contribute equally to the action. In fact, not all human joints are informative for action recognition

and some irrelevant joints will bring in noise information. Therefore, Liu et al. [48] utilized an attention mechanism to capture the important human joints, and proposed a global context-aware attention LSTM to model human motion on the human joints with different attention factors.

## 2.2 Human-Skeleton Motion Prediction

Human-skeleton motion prediction aims to generate the future motions based on the observed human motions, which is becoming an attractive topic in the area of computer vision. It motivates a wide spectrum of applications, such as athletic performance analysis, surveillance, man-machine interfaces, somatic game, Virtual Reality (VR), and so on [49]. Generally, the human-skeleton motion data is captured by a MOCAP device, e.g., Kinect, Vicon. At present, there are some human-skeleton motion datasets released on websites, such as H3.6m mocap dataset (H3.6M) [50], CMU mocap database<sup>2</sup>. In particular, the H3.6M mocap dataset is the largest-scale and available human skeleton dataset for evaluating human skeleton prediction.

In the early stage, since human motion is sequential and nonlinear over time, some researchers utilized various probabilistic models, e.g., latent variable model [9], Markov model [3], [10], generative model [11], and Gaussian process dynamical model [51], to predict the future human motion sequence based on the historical human motions. For example, Taylor et al. [11] proposed non-linear generative model to utilize an undirected model with binary latent variables and real-valued “visible” variables to represent joint angles. Lehrmann et al. [3] proposed a non-parametric and nonlinear Markov model instead of simple Markov models for flexibly inferring future motions.

2. <http://mocap.cs.cmu.edu/>

Recently, witnessing the powerful ability of RNN in the action recognition task, some researchers proposed various variants of RNN to model the human-skeleton motion based on an observed motion sequence [1], [18], [19], [52], which outperformed conventional methods on the motion prediction task. Fragkiadaki et al. [18] first employ RNN model to address the problem of human motion predictions. The authors proposed an Encoder-Recurrent-Decoder (ERD) model to encode and decode human motions by incorporating nonlinear encoder and decoder networks before and after recurrent layers. However, ERD is prone to accumulate errors, and quickly produces unrealistic human motion, though an added noise scheduling can reduce such errors to some extent. Subsequently, Martinez et al. [1] embedded the residual module in the single-layer GRU architecture to model first-order motion derivatives. One limitation is that these methods pay no attention to the dependence of some joints in the spatial space. In fact, two neighboring joints in a frame usually have the coherent motion direction. Based on this, Jain et al. [19] extend a spatio-temporal graph to a structural RNN, in which each node denotes a human joint, and the adjacency of graph between two nodes (joints) describe the dependence of two joints. This motivates us to model human motions in both the spatial and temporal spaces.

The above RNN-based human motion prediction methods use the last motion and the current input motion to decide the future motion, this may be bring in noise motion information when the last motion is a sudden motion that is not consistent with the previous motions, or the last motion is not inaccurate enough. Therefore, Tang et al. [20] considered using all historical motions instead of the last motion to predict the next motion in the RNN model. Specifically, they presented an attention mechanism to assign all useful historical motions with different attention factors based on their contributions to prediction of the next motion. Inspired by this, we further consider embedding the attention mechanism into RNN to model human motions in both of the spatial and temporal spaces.

### 3 METHODOLOGY

#### 3.1 Background and Idea

Let  $\mathbf{x}_t$  denote a representation of the human-skeleton motion in frame  $t$  and  $\{\mathbf{x}_t\}_{t=1}^T$  denote an observed human-skeleton sequence  $\mathcal{S}$ , as shown in Table 1, the goal of human-skeleton motion prediction is to generate the future human-skeleton motion  $\{\tilde{\mathbf{x}}_{t'}\}_{t'=1}^{T'}$  close to the ground-truth skeleton motion  $\{\tilde{\mathbf{x}}_t\}_{t=1}^T$  as much as possible. Some conventional works [1], [18] utilized Recurrent Neural Network (RNN) to predict human motion  $\tilde{\mathbf{x}}_{t'+1}$  at the future time step  $(t'+1)$  by the last motion state  $\mathbf{h}_{t'-1}$  and the last predicted motion  $\tilde{\mathbf{x}}_{t'}$ , as follows,

$$\tilde{\mathbf{x}}_{t'+1} := \text{RNN}(\tilde{\mathbf{x}}_{t'}, \mathbf{h}_{t'-1}), \quad (1)$$

The final motion state and human motion  $\mathbf{x}_T$  of observed human motions are denoted by  $\mathbf{h}_0$  and  $\tilde{\mathbf{x}}_0$  when predicting the skeleton motion  $\tilde{\mathbf{x}}_1$ .

If there is a sudden motion in the last time step, the normal motion information will be disturbed or some noise

TABLE 1  
Notations and definitions.

Notation	Definition
$t \in \{1, 2, \dots, T\}$	Index of the observed motion sequence.
$t' \in \{1, 2, \dots, T'\}$	Index of the future motion sequence.
$\mathbf{x}_t$	Observed skeleton sequence at historical time step $t$ .
$\tilde{\mathbf{x}}_{t'}$	Predicted motion at future time step $t'$ .
$\tilde{\mathbf{x}}_{t'}$	Ground-truth motion at future time step $t'$ .
$k \in \{1, 2, \dots, K\}$	Index of the observed joint sequence.
$\mathbf{F}$	Skeleton-joint feature map covering $\{1, \dots, T\}$ .
$\mathbf{F}_{t'}^a$	Skeleton-attention feature map covering $\{1, \dots, T, t'\}$ .
$\mathbf{F}_{t'}^j$	Skeleton-joint feature map covering $\{1, \dots, T, t'\}$ .
$\mathbf{F}_{co}^{t'}$	Skeleton-joint co-attention feature map covering $\{1, \dots, T, t'\}$ .

information will be brought in. Therefore, we can use all information motion information to predict the future motion  $\tilde{\mathbf{x}}_{t'+1}$  by RNN [20], i.e.,

$$\tilde{\mathbf{x}}_{t'+1} := \text{RNN}(\tilde{\mathbf{x}}_{t'}, \text{Attention}(\{\mathbf{x}_t\}_{t=1}^T)). \quad (2)$$

where  $\text{Attention}(\cdot)$  indicates an attention mechanism that computes the attention factors of all historical skeletons in the temporal space. Different historical motions are weighted by the different attention factors due to their contributions to the prediction of future motion at time step  $(t'+1)$ . In the other words, the more important skeleton motion will be assigned the larger attention factor.

However, the learning model in Eq. (2) ignores the spatial coherence among joints in the spatial space. For example, two neighboring joints in the spatial space usually have the similar motion direction. Therefore, we design a new **Spatiotemporal Co-Attention (SCA)** mechanism to compute the spatial-attention factors and the temporal-attention factors corresponding to joints in the spatial space and skeletons in the temporal space, respectively. The learning model of Eq. (3) can be embedded with SCA as follows,

$$\tilde{\mathbf{x}}_{t'+1} := \text{RNN}(\tilde{\mathbf{x}}_{t'}, \text{SCA}(\mathcal{S})). \quad (3)$$

Based on this, we propose a novel **Spatiotemporal Co-attention Recurrent Neural Networks (SC-RNN)** to capture the spatial coherence among joints and the temporal evolution among skeletons simultaneously by utilizing all useful historical motion information as the motion context. SC-RNN mainly consists of a Spatial Attention GRU, a Temporal Attention GRU, a spatial confidence gate, and a weighted gram matrix-based loss, as shown in Figure 2. The details of SC-RNN will be introduced in the following sections.

#### 3.2 Skeleton-joint Co-attention Attention (SCA)

In this work, a human motion  $\mathbf{x}_t$  at time step  $t$  is represented by the human skeleton at this time step by concatenating the 3D location parameters of all  $K$  joints in the angle axis. For one observed human motion sequence  $\mathcal{S} = \{\mathbf{x}_t \in \mathbb{R}^{d \times T}\}_{t=1}^T$ , we can define a **skeleton-joint feature map**  $\mathbf{F} \in \mathbb{R}^{d \times T}$  (where  $d = 3 \times K$ ) covering all the historical time steps  $\{1, \dots, T\}$ , as follows,

$$\mathbf{F}_{(:,j)} \triangleq \mathbf{x}_j, \quad j = 1, 2, \dots, T, \quad (4)$$

where  $\mathbf{F}_{(:,j)}$  denotes the  $j$ -th column of  $\mathbf{F}$ . One row and column of  $\mathbf{F}$  indicates a joint-type feature and skeleton-type

feature of human motion in the spatial and temporal spaces, respectively.

As mentioned before, one long-term motion at the future time step can be well predicted by the current motion information, as well as all the observed motion information (i.e., motion context). However, not all observed skeleton motions equally contribute to the prediction of the motion at one future time step. If one observed motion is considerably consistent with one future motion, it could contribute a lot to predicting this future motion, and should be integrated into the motion context with a larger degree. Therefore, how to measure the consistency between an observed motion  $\mathbf{x}_t$  and the future motion  $\tilde{\mathbf{x}}_{t'}$  is the key. Inspired by the attention models in previous works [20], [53], we adopt an attention mechanism to measure the consistency between the observed skeleton motion  $\mathbf{F}_{(:,j)}$  and the predicted skeleton-motion state  $\mathbf{h}_{t'-1} \in \mathbb{R}^d$  at time step  $(t' - 1)$ , since  $\tilde{\mathbf{x}}_{t'}$  is unknown. Specifically, the skeleton-attention module of Skeleton-joint Co-Attention (SCA) in temporal space is formulated as follows,

$$\beta_j^e = \mathbf{w}_e^T \cdot \varphi(\mathbf{U}_{eh}\mathbf{h}_{t'-1} + \mathbf{U}_{ef}\mathbf{F}_{(:,j)} + \mathbf{b}_e); \quad (5)$$

$$\{\alpha_j^e\}_{j=1}^T = \text{softmax}(\{\beta_j^e\}_{j=1}^T, \tau_1), \quad (6)$$

where  $\tau_1$  is a temperature parameter of the softmax function [53],  $\varphi$  is a hyperbolic tangent, i.e.,  $\tanh(\cdot)$ , the superscript notation  $T$  is the transposition operator of a vector/matrix,  $\mathbf{U}_{e*}$  is the weight matrix,  $\mathbf{w}_e$  is a weight vector, and  $\mathbf{b}_e$  is a bias vector.

After obtaining the skeleton-attention factor  $\alpha_j^e$ , the **skeleton-attention feature map**  $\mathbf{F}_a^{t'}$  and skeleton-attention feature  $\mathbf{h}_a^{t'}$  (i.e., the **skeleton motion context**) at time step  $t'$  can be calculated as follows,

$$\begin{aligned} \mathbf{F}_a^{t'}(:,j) &= \alpha_j^e \cdot \mathbf{F}_{(:,j)}; \\ \mathbf{h}_a^{t'} &= \frac{1}{T} \sum_{j=1}^T \mathbf{F}_a^{t'}(:,j). \end{aligned} \quad (7)$$

By integrating the skeleton motion context  $\mathbf{h}_a^{t'}$ , a new **skeleton-attention network** is formulated as follows,

$$\mathbf{z}_{t'} = \sigma(\mathbf{W}_{zx}\tilde{\mathbf{x}}_{t'} + \mathbf{W}_{zh}\mathbf{h}_{t'-1} + \mathbf{W}_{za}\mathbf{h}_a^{t'} + \mathbf{b}_z); \quad (8)$$

$$\mathbf{r}_{t'} = \sigma(\mathbf{W}_{rx}\tilde{\mathbf{x}}_{t'} + \mathbf{W}_{rh}\mathbf{h}_{t'-1} + \mathbf{W}_{ra}\mathbf{h}_a^{t'} + \mathbf{b}_r); \quad (9)$$

$$\mathbf{c}_{t'} = \varphi(\mathbf{W}_{cx}\tilde{\mathbf{x}}_{t'} + \mathbf{W}_{ch}(\mathbf{r}_{t'} \odot \mathbf{h}_{t'-1}) + \mathbf{b}_c); \quad (10)$$

$$\mathbf{h}_{t'} = (1 - \mathbf{z}_{t'}) \odot \mathbf{h}_{t'-1} + \mathbf{z}_{t'} \odot \mathbf{c}_{t'}, \quad t' = 1, \dots, T', \quad (11)$$

where  $\mathbf{z}_{t'}$ ,  $\mathbf{r}_{t'}$ ,  $\mathbf{c}_{t'}$ , and  $\mathbf{h}_{t'}$   $\in \mathbb{R}^d$  are the update gate, reset gate, memory, and skeleton motion state at time step  $t'$  respectively,  $\sigma(\cdot)$  is a sigmoid function,  $\odot$  denotes the element-wise product,  $\varphi(\cdot)$  is a hyperbolic tangent  $\tanh(\cdot)$ ,  $\mathbf{W}_{*x}$  and  $\mathbf{W}_{*h}$  are weight matrices, and  $\mathbf{b}_*$  is bias vector. Figure 3 shows the detailed architecture of skeleton-attention network.

Empirically, for the  $k$ -th joint covering the time steps  $\{1, \dots, T, t'\}$ , its motion is coherent to some other joints with different degrees in spatial space. Such as, the coherent motions of leg joint and hand joint in a ‘‘walking’’. Therefore, it is crucial for measuring the coherence between the  $k$ -th joint motion and its neighboring joints. Similar to skeleton-attention module, we also adopt an attention

mechanism to measure the coherence degree of the  $k$ -th joint motion and the  $l$ -th joint motion covering the time steps  $\{1, \dots, T, t'\}$ , where  $l = 1, 2, \dots, K$ , and  $l \neq k$ . Specifically, we first define a skeleton-joint feature map  $\mathbf{F}^{t'} \in \mathbb{R}^{d \times (T+1)}$  covering the time steps  $\{1, \dots, T, t'\}$ , i.e.,

$$\mathbf{F}^{t'} \triangleq [\mathbf{F}, \mathbf{h}_{t'}], \quad t' = 1, 2, \dots, T', \quad (12)$$

where  $\mathbf{h}_{t'}$  is obtained by the skeleton-attention network. Subsequently, the joint-attention module of SCA can be expressed as below,

$$\beta_l^k = \mathbf{w}_c^T \cdot \varphi(\mathbf{U}_{cb} \cdot \mathbf{M}_k^{t'} \cdot \mathbf{1} + \mathbf{U}_{cm} \cdot \mathbf{M}_l^{t'} \cdot \mathbf{1} + \mathbf{b}_l), \quad (13)$$

where  $\mathbf{1} \in \mathbb{R}^{T+1}$  denotes a vector with all elements being set to 1, and we set  $k_* = 3 \times (k - 1) + *$ ,  $l_* = 3 \times (l - 1) + *$ ,  $* = 1, 2, 3$ ,  $\mathbf{M}_k^{t'} = [\mathbf{F}_{(k_1, :)}^{t'}; \mathbf{F}_{(k_2, :)}^{t'}; \mathbf{F}_{(k_3, :)}^{t'}]$ , and  $\mathbf{M}_l^{t'} = [\mathbf{F}_{(l_1, :)}^{t'}; \mathbf{F}_{(l_2, :)}^{t'}; \mathbf{F}_{(l_3, :)}^{t'}]$  for brevity. A joint-attention factor  $\alpha_l^k$  of the  $l$ -th joint corresponding to the  $k$ -th joint can be computed as below,

$$\{\alpha_l^k\}_{l=1, l \neq k}^K = \text{softmax}(\{\beta_l^k\}_{l=1, l \neq k}^K, \tau_2), \quad (14)$$

where  $\tau_2$  is a temperature parameter of softmax.

For the  $k$ -th joint, if we obtain  $\{\alpha_l^k\}_{l=1, l \neq k}^K$ , we can compute a **skeleton-joint co-attention feature map**  $\mathbf{F}_{co}^{t'}$  of  $\mathbf{F}^{t'}$  of the skeleton attention feature map  $\mathbf{F}_a^{t'}$  in spatiotemporal space, i.e.,

$$\mathbf{F}_{co(l_*, :)}^{t'} = \alpha_l^k \cdot [\mathbf{F}_a^{t'}(l_*, 1:T), \mathbf{F}_a^{t'}(l_*, \text{end})], \quad * = 1, 2, 3, \quad (15)$$

where  $l = 1, \dots, K$ , and  $l \neq k$ . In this way, each element  $\mathbf{F}_{co(i,j)}^{t'}$  ( $j = 1, 2, \dots, T$ ) is assigned with a **skeleton-joint attention factor**, where one skeleton-joint attention factor is obtained through multiplying a skeleton-attention factor by a joint attention factor. Then the **co-attention motion context**  $\mathbf{O}_k^{t'}$  of the  $k$ -th joint covering the time steps  $\{1, 2, \dots, T, t'\}$  can be calculated as follows

$$\mathbf{q}_k^{*'} \triangleq \frac{1}{K-1} \sum_{l=1, l \neq k}^K \mathbf{F}_{co(3 \times (l-1) + *, :)}^{t'}, \quad * = 1, 2, 3, \quad (16)$$

$$\mathbf{O}_k^{t'} \triangleq [\mathbf{q}_k^{1'}; \mathbf{q}_k^{2'}; \mathbf{q}_k^{3'}].$$

Similar to the skeleton-attention network, we can formulate a **spatial-attention network** to learn the human-joint motion state  $\mathbf{Q}_s^{t'}$  by integrating the co-attention motion context  $\mathbf{O}_s^{t'}$  in a sequence  $\{1, 2, \dots, s, \dots, S\}$ ,

$$\mathbf{Z}_s^{t'} = \sigma(\mathbf{W}_{zm}\mathbf{M}_s^{t'} + \mathbf{W}_{zq}\mathbf{Q}_{s-1}^{t'} + \mathbf{W}_{zo}\mathbf{O}_s^{t'} + \mathbf{B}_z); \quad (17)$$

$$\mathbf{R}_s^{t'} = \sigma(\mathbf{W}_{rm}\mathbf{M}_s^{t'} + \mathbf{W}_{rq}\mathbf{Q}_{s-1}^{t'} + \mathbf{W}_{ro}\mathbf{O}_s^{t'} + \mathbf{B}_r); \quad (18)$$

$$\mathbf{C}_s^{t'} = \varphi(\mathbf{W}_{cm}\mathbf{M}_s^{t'} + \mathbf{W}_{cq}(\mathbf{R}_s^{t'} \odot \mathbf{Q}_{s-1}^{t'}) + \mathbf{B}_c); \quad (19)$$

$$\mathbf{Q}_s^{t'} = (1 - \mathbf{Z}_s^{t'}) \odot \mathbf{Q}_{s-1}^{t'} + \mathbf{Z}_s^{t'} \odot \mathbf{C}_s^{t'}, \quad s = 1, \dots, S, \quad (20)$$

where  $\mathbf{M}_s^{t'}$ ,  $\mathbf{Z}_s^{t'}$ ,  $\mathbf{R}_s^{t'}$ ,  $\mathbf{C}_s^{t'}$ , and  $\mathbf{Q}_s^{t'}$  are the input joint motion, update gate, reset gate, memory, and the joint motion state, respectively.  $s$  is the index of in a pre-defined travel-based joint sequence  $\Omega = \{1, 2, \dots, s, \dots, S\}$  [22]. Intuitively, we can predefine the spatial joint sequence according to the ID number of the joint and update all joints by Eq. (17)~(20), namely ID-based sequence. However, such joint sequence did not consider the joint structure.

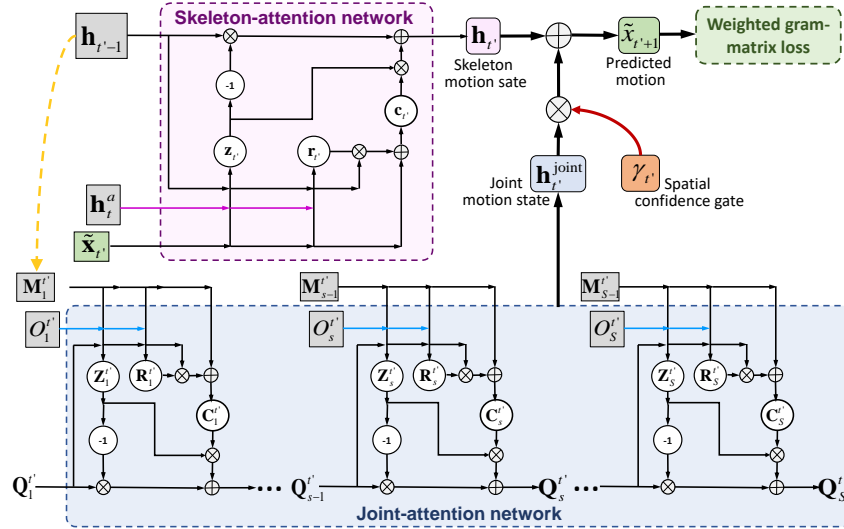


Fig. 3. Architecture of SC-GRU (a GRU version of the proposed SC-RNN) at time step  $t'$ . SC-RNN mainly consists of the skeleton-attention network and joint-attention network, which simultaneously model the skeleton motion and joint motion.

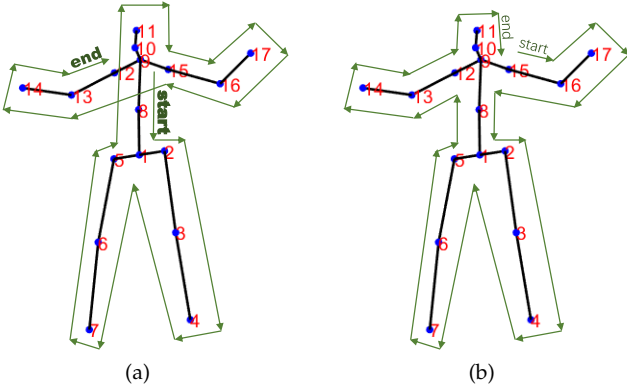


Fig. 4. Different orders for spatial arrangement. (a) and (b) represent the traveling-based and surrounding-based sequences, respectively.

In some previous works [22], [54], the traveling-based and surrounding-based joint sequences are better to describe the human body structure, and achieve the better performance compared with the traditional ID-based sequence in terms of action recognition. Therefore, we also adopt the traveling-based and surrounding-based sequences in this work. Specifically, the traveling-based and surrounding-based sequences are drawn in Figure 4, where the traveling-based and surrounding-base sequences are  $\{9, 8, 1, 2, 3, 4, 3, 2, 1, 5, 6, 7, 6, 5, 1, 8, 9, 10, 11, 10, 9, 15, 15, 17, 16, 15, 9, 12, 13, 14, 13, 12, 9\}$ , and  $\{9, 15, 16, 17, 16, 15, 9, 8, 1, 2, 3, 4, 3, 2, 1, 5, 6, 7, 6, 5, 1, 8, 9, 12, 13, 14, 13, 12, 9, 10, 11, 10, 9\}$ , respectively.

### 3.3 Skeleton-joint Co-Attention GRU (SC-GRU)

Till now, we can integrate the skeleton-attention network and joint-attention network into a Skeleton-joint Co-attention GRU (SC-GRU), namely a GRU version of the proposed SC-RNN<sup>3</sup>. Figure 3 shows the architecture of SC-

3. The other versions of SC-RNN (such as SC-RNN, SC-LSTM) can be easily formulated in the same way.

GRU. In SC-GRU, at time step  $t'$ , we first obtain the skeleton motion state  $\mathbf{h}_{t'}$  based on the human skeletons, and then update each joint to obtain  $\mathbf{Q}_k^{t'}$  in spatiotemporal space. Finally, the predicted motion  $\tilde{\mathbf{x}}_{t'+1}$  at time step  $(t' + 1)$  can be expressed as

$$\tilde{\mathbf{x}}_{t'+1} = \frac{1}{2}(\mathbf{h}_{t'} + \gamma_{t'} \odot \mathbf{h}_{t'}^{joint}), \quad (21)$$

where  $\mathbf{h}_{t'}^{joint} = [\mathbf{Q}_1^{t'(:,end)}; \mathbf{Q}_2^{t'(:,end)}; \dots; \mathbf{Q}_K^{t'(:,end)}]$ .  $\gamma_{t'}$  is a spatial confidence gate at time step  $t'$ , which is activated by the difference between the predicted joint motion state  $\mathbf{h}_{t'}^{joint}$  and the input joint motion  $\mathbf{m}_{t'}^{joint} = [\mathbf{M}_1^{t'(:,end)}; \mathbf{M}_2^{t'(:,end)}; \dots; \mathbf{M}_K^{t'(:,end)}]$ , as follows

$$\begin{aligned} \mathbf{f}_h^{t'} &= \varphi(\mathbf{W}_{fh} \mathbf{h}_{t'}^{joint} + \mathbf{b}_h); \\ \mathbf{f}_m^{t'} &= \varphi(\mathbf{W}_{fm} \mathbf{m}_{t'}^{joint} + \mathbf{b}_m); \\ \gamma_{t'} &= \chi(\mathbf{f}_h^{t'} - \mathbf{f}_m^{t'}), \end{aligned} \quad (22)$$

where  $\chi(\theta) = \frac{1}{\exp(\rho\theta^2)}$  is an element-wise activation function,  $\rho$  is a parameter to control the bandwidth of the activation function. In Eq. (22), if the obtained joint motion state differs from the input joint motion state, the former has a lower confidence, and will be suppressed in the updating of the predicted motion  $\tilde{\mathbf{x}}_{t'+1}$  in Eq. (21).

### 3.4 Weighted gram-matrix loss

On the top of the SC-GRU, there is a loss function to measure the difference between the predicted motion and the ground-truth motion. Conventional methods [1], [18], [19] usually adopt Mean Square Error (MSE) as the loss function to minimize the errors between the predicted motion and ground truth in the model learning. However, MSE treats all predicted motions independently, which ignores the relation between motions at different time steps, and causes motion inconsistency to some extent. Recently, a gram-matrix loss instead of MSE is proposed to produce highly correlated human motion in temporal space [20]. However, it only considers the correlation between motions in two consecutive

frames. Therefore, we extend the gram-matrix loss to a new weighted gram-matrix loss, as follows

$$\mathcal{L} = \frac{1}{T} \sum_{t'=1}^{T'} \|(\mathcal{G}(\tilde{\mathbf{x}}_{t'}) - \mathcal{G}(\hat{\mathbf{x}}_{t'}))\|_F^2, \quad (23)$$

where  $\mathcal{G}(\tilde{\mathbf{x}}_{t'})$  and  $\mathcal{G}(\hat{\mathbf{x}}_{t'})$  are gram matrices corresponding to  $\tilde{\mathbf{x}}_{t'}$  and  $\hat{\mathbf{x}}_{t'}$ , respectively, defined as

$$\mathcal{G}(\tilde{\mathbf{x}}_{t'}) \triangleq [\mathbf{I}_{1,t'}\tilde{\mathbf{x}}_1; \mathbf{I}_{2,t'}\tilde{\mathbf{x}}_2; \cdots; \mathbf{I}_{t'-1,t'}\tilde{\mathbf{x}}_{t'-1}; \tilde{\mathbf{x}}_{t'}] \times [\mathbf{I}_{1,t'}\tilde{\mathbf{x}}_1; \mathbf{I}_{2,t'}\tilde{\mathbf{x}}_2; \cdots; \mathbf{I}_{t'-1,t'}\tilde{\mathbf{x}}_{t'-1}; \tilde{\mathbf{x}}_{t'}]^T; \quad (24)$$

$$\mathcal{G}(\hat{\mathbf{x}}_{t'}) \triangleq [\mathbf{I}_{1,t'}\hat{\mathbf{x}}_1; \mathbf{I}_{2,t'}\hat{\mathbf{x}}_2; \cdots; \mathbf{I}_{t'-1,t'}\hat{\mathbf{x}}_{t'-1}; \hat{\mathbf{x}}_{t'}] \times [\mathbf{I}_{1,t'}\hat{\mathbf{x}}_1; \mathbf{I}_{2,t'}\hat{\mathbf{x}}_2; \cdots; \mathbf{I}_{t'-1,t'}\hat{\mathbf{x}}_{t'-1}; \hat{\mathbf{x}}_{t'}]^T. \quad (25)$$

In Eq. (24) and (25),  $\mathbf{I} \in \mathbb{R}^{T' \times T'}$  is a coefficient matrix to measure the correction between two skeleton motions at different time steps, i.e.,

$$\mathbf{I}_{i,j} = \exp\left(-\frac{\|\hat{\mathbf{x}}_i - \tilde{\mathbf{x}}_j\|_2^2}{\tau^2}\right), \quad i, j = 1, 2, \dots, T', \quad (26)$$

where  $\tau$  is a parameter of the RBF kernel.

## 4 EXPERIMENTS

We conduct experiments on human motion prediction to evaluate the performance of the proposed SC-RNN compared with the state-of-the-art methods.

### 4.1 Dataset

Following previous works [1], [20], we select the H3.6m mocap dataset (H3.6M) [50] to evaluate the performance of the proposed SC-RNN in the experiments. H3.6M is the largest available human-skeleton motion dataset captured, which is appropriate for training deep network with a huge number of parameters. It includes 15 actions are performed by seven different actors, i.e., “directions”, “discussion”, “eating”, “greeting”, “phoning”, “posing”, “purchases”, “sitting”, “sittingdown”, “smoking”, “takingphoto”, “waiting”, “walking”, “walkingdog”, and “walkingtogether”. Some actions are periodic actions, e.g., “walking”, and the other ones are non-periodic, e.g., “taking photo”. For each action, actor, and camera viewpoint, there are two video sequences, each of which has 3000 ~ 5000 frames. Each human-skeleton sequence records the 3D locations of 32 joints at each frame. Since many of joints are very close in the 3D angle axis, we select 17 representative joints of each skeleton, which provide enough details of human motion.

### 4.2 Experimental Setting

For fair comparison, following setting in [1], [18], [19], five actors’ motions are selected for testing, while the rest ones for training. Each human joint is represented by a three-dimensional location vector in the 3D angle axis [11]. Thus a human skeleton at one time step is represented by concatenating all locations of all joints. For each human-skeleton sequence, we take two seconds of motion as the observed ones to predict the future 400ms and 1000ms motion for short-term and long-term motion prediction, respectively.

Following the evaluation in previous works [1], [19], [20], we adopt the Mean Angle Error (MAE) as the evaluation criteria, which measure the Euclidean distance between

TABLE 2  
Mean Angle Error obtained by SC-RNN with different sequence strategies.

Strategies	Short-term		Long-term	
	80ms	400ms	720ms	1000ms
ID-based sequence	0.40	1.06	1.20	1.50
Surrounding-based sequence	0.39	<b>1.03</b>	1.18	1.48
Traveling-based sequence	<b>0.37</b>	1.04	<b>1.17</b>	<b>1.46</b>

the predicted joints and its ground-truth in the 3D angle axis.

In the configuration of SC-RNN, the number of memory cell nodes is set to 1024. We use PyTorch toolbox and a NVIDIA Tesla K20 GPU to run the experiments. The learning rate, decay rate, momentum and batch size are set to  $0.5 \times 10^{-3}$ , 0.95, 0.9 and 32, respectively.

In SA-GRU, we introduced traveling-based sequence and surrounding-based sequences, as shown in Figure 4. These two sequences have shown the competitive performance in the task of human action recognition [22], [54]. For the task of human motion prediction, we firstly explore the better sequence strategy by conducting the experiments based on three sequences, namely ID-based sequence, traveling-based sequence and surrounding-based sequences. The compared results are reported in Table 2. It can be seen that the SC-RNN with traveling-based sequence achieves the best performance. Since two neighboring joints have the consistent motion direction, the adjacency information between any the two neighboring joints in the traveling-based will be better maintained. In the following experiments, SC-RNN is selected the traveling-based sequence by default.

### 4.3 Ablation studies

To illustrate the novelty of SC-RNN, we conduct ablation studies between SC-RNN and baseline methods. 1) **SC-RNN w/o SCA**: it throws away the Skeleton-joint Co-attention Attention (SCA) in SC-RNN. 2) **SC-RNN w/o skeleton attention**: it throws away the skeleton-attention module, namely  $\{\alpha_j^e\}_{j=1}^T$  are setting to 1. 3) **SC-RNN w/o joint attention**: it throws away the joint-attention module, namely  $\{\alpha_l^k\}_{l=1, l \neq k}^K$  are setting to 1.

Table 3 shows the average MAE of the proposed SC-RNN compared with the baselines on all 15 actions in the H3.6M dataset. we can see that SC-RNN outperforms all baseline methods. Specifically, “SC-RNN w/o skeleton attention” and “SC-RNN w/o joint attention” improve performance of “SC-RNN w/o SCA” without attention mechanism to some extent. In particular, the MAE achieved by “SC-RNN w/o skeleton attention” is comparable to “SC-RNN w/o joint attention”, where both of them adopt the attention mechanism in a single space. SC-RNN with SCA in spatiotemporal space outperforms “SC-RNN w/o skeleton attention” and “SC-RNN w/o joint attention” embedded with the “single-attention” module in a single space. Overall, it can be concluded that SCA mechanism is more effective than a “single-attention” mechanism in modeling human motions.

TABLE 3

Performance comparison among different methods in terms of short-term and long-term human motion prediction for all 15 actions on the H3.6m dataset.

Methods	Short-term motion prediction				Long-term motion prediction			
	80ms	160ms	320ms	400ms	560ms	640ms	720ms	1000ms
ERD [18]	0.60	0.85	1.15	1.36	1.54	1.63	1.70	1.80
LSTM-3LR [18]	0.56	0.80	1.11	1.33	1.49	1.58	1.66	1.75
Res-GRU [1]	0.40	0.70	1.06	1.18	1.37	1.43	1.53	1.63
MHU [20]	0.37	0.65	0.97	1.10	1.26	1.35	1.43	1.54
SC-RNN w/o SCA	0.49	0.72	0.97	1.20	1.29	1.40	1.46	1.52
SC-RNN w/o skeleton attention	0.36	<b>0.60</b>	0.92	1.06	1.24	1.35	1.41	1.51
SC-RNN w/o joint attention	<b>0.36</b>	0.59	0.95	1.03	1.20	1.38	<b>1.34</b>	1.49
SC-RNN	0.37	0.62	<b>0.92</b>	<b>1.04</b>	<b>1.17</b>	<b>1.25</b>	1.36	<b>1.46</b>

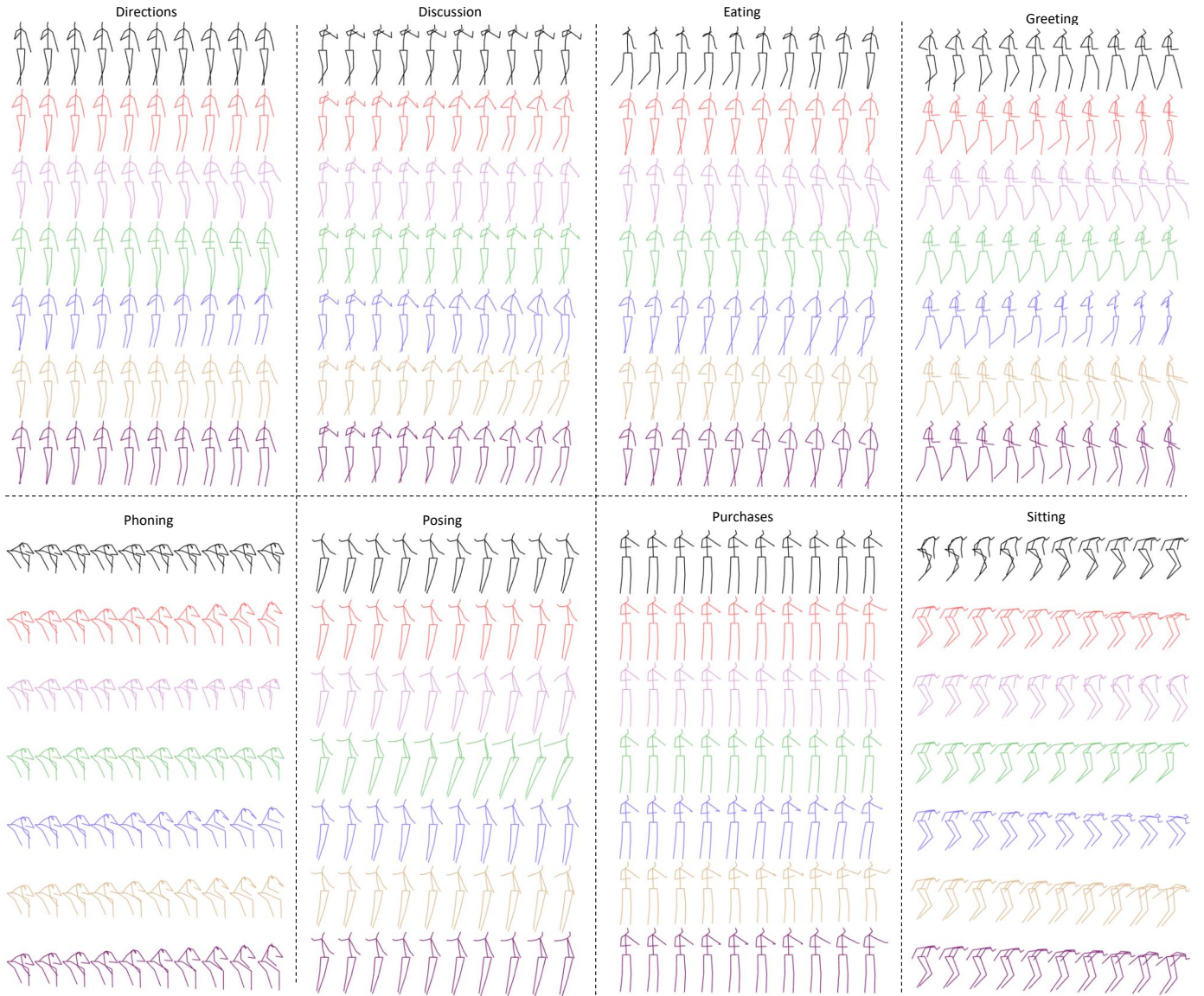


Fig. 5. Some visualized results of the motion prediction for all 15 actions. In each group, the first and the second rows are the observed motion and the ground-truth human motions, respectively; and the 3rd-7th rows are the human motion predicted by ERD [18], LSTM-3LR [18], Res-GRU [1], MHU [20] and the proposed SC-RNN, respectively. For better view, please see  $\times 3$  original color PDF. This figure is followed by Figure 6.

#### 4.4 Comparison with the competitive methods

To illustrate the superiority of the proposed SC-RNN, we compare SC-RNN with several related methods, including

TABLE 4  
Performance comparison among different methods for each human action via mean angle error.

Methods	Directions								Discussion							
	Short-term motion prediction				Long-term motion prediction				Short-term motion prediction				Long-term motion prediction			
	80ms	160ms	320ms	400ms	560ms	640ms	720ms	1000ms	80ms	160ms	320ms	400ms	560ms	640ms	720ms	1000ms
ERD [18]	0.77	0.83	0.94	1.03	1.12	1.16	1.22	1.35	0.89	0.97	1.23	1.74	1.80	1.80	1.89	1.97
LSTM-3LR [18]	0.60	0.75	0.82	0.97	1.06	1.10	1.17	1.23	0.81	0.90	1.12	1.64	1.75	1.67	1.85	1.93
Res-GRU [1]	0.32	0.52	0.77	0.89	0.96	1.04	1.09	1.13	0.36	0.70	1.01	1.09	1.56	1.65	1.75	1.91
MHU [20]	0.30	<b>0.51</b>	0.76	0.84	0.91	0.93	<b>0.97</b>	1.08	<b>0.32</b>	0.68	0.95	<b>1.02</b>	1.34	1.52	1.66	1.90
SC-RNN	<b>0.30</b>	0.52	<b>0.69</b>	<b>0.79</b>	<b>0.87</b>	<b>0.93</b>	1.01	<b>1.07</b>	0.33	<b>0.67</b>	<b>0.94</b>	1.05	<b>1.27</b>	<b>1.49</b>	<b>1.56</b>	<b>1.86</b>
Methods	Eating								Greeting							
	Short-term motion prediction				Long-term motion prediction				Short-term motion prediction				Long-term motion prediction			
	80ms	160ms	320ms	400ms	560ms	640ms	720ms	1000ms	80ms	160ms	320ms	400ms	560ms	640ms	720ms	1000ms
ERD [18]	0.73	0.78	0.84	0.93	1.02	1.07	1.11	1.15	1.07	1.33	1.67	1.84	2.39	2.31	2.34	2.39
LSTM-3LR [18]	0.69	0.74	0.80	0.87	0.91	0.98	1.03	1.09	1.03	1.32	1.79	1.89	2.31	2.28	2.31	2.36
Res-GRU [1]	0.27	0.44	0.64	0.82	0.88	0.94	1.00	1.02	0.69	1.10	1.61	1.73	2.13	1.89	1.86	2.00
MHU [20]	0.25	0.46	0.61	0.72	0.77	0.81	0.87	0.90	0.56	0.91	1.36	1.51	1.79	1.77	1.82	1.88
SC-RNN	<b>0.25</b>	<b>0.42</b>	<b>0.56</b>	<b>0.68</b>	<b>0.67</b>	<b>0.73</b>	<b>0.80</b>	<b>0.87</b>	<b>0.54</b>	<b>0.79</b>	<b>1.13</b>	<b>1.31</b>	<b>1.49</b>	<b>1.34</b>	<b>1.63</b>	<b>1.64</b>
Methods	Phoning								Posing							
	Short-term motion prediction				Long-term motion prediction				Short-term motion prediction				Long-term motion prediction			
	80ms	160ms	320ms	400ms	560ms	640ms	720ms	1000ms	80ms	160ms	320ms	400ms	560ms	640ms	720ms	1000ms
ERD [18]	0.47	0.68	0.89	0.93	1.07	1.13	1.21	1.27	0.56	1.01	1.25	1.57	1.89	2.11	2.23	2.59
LSTM-3LR [18]	0.39	0.52	0.74	0.90	1.01	1.07	1.15	1.23	0.57	1.02	1.45	1.91	1.93	2.16	2.38	2.67
Res-GRU [1]	0.27	0.46	0.69	0.82	0.95	1.04	1.10	1.16	0.41	0.79	1.11	1.28	1.81	1.77	2.26	2.57
MHU [20]	0.29	0.45	0.67	0.71	0.89	0.97	1.08	1.14	<b>0.32</b>	<b>0.62</b>	1.21	1.48	<b>1.80</b>	<b>2.08</b>	<b>2.17</b>	<b>2.51</b>
SC-RNN	<b>0.27</b>	<b>0.43</b>	<b>0.62</b>	<b>0.68</b>	<b>0.79</b>	<b>0.81</b>	<b>1.01</b>	<b>1.08</b>	0.34	0.67	<b>1.20</b>	<b>1.45</b>	1.86	2.11	2.20	2.53
Methods	Purchases								Sitting							
	Short-term motion prediction				Long-term motion prediction				Short-term motion prediction				Long-term motion prediction			
	80ms	160ms	320ms	400ms	560ms	640ms	720ms	1000ms	80ms	160ms	320ms	400ms	560ms	640ms	720ms	1000ms
ERD [18]	0.76	0.89	0.98	1.12	1.26	1.35	1.40	1.57	0.44	0.93	1.24	1.59	1.74	1.96	2.01	2.10
LSTM-3LR [18]	0.71	0.84	0.93	1.10	1.22	1.36	1.47	1.58	0.45	0.91	1.39	1.59	1.69	1.90	1.97	2.03
Res-GRU [1]	0.51	0.97	1.08	1.17	1.21	1.28	1.36	1.46	0.44	0.91	1.49	1.64	1.71	1.82	1.91	1.97
MHU [20]	0.48	0.96	1.09	1.12	1.18	1.24	1.30	1.37	0.44	0.89	1.12	1.34	1.56	1.67	1.78	1.84
SC-RNN	<b>0.47</b>	<b>0.93</b>	<b>1.07</b>	<b>1.13</b>	<b>1.17</b>	<b>1.24</b>	<b>1.30</b>	<b>1.30</b>	<b>0.43</b>	<b>0.89</b>	<b>1.12</b>	<b>1.34</b>	<b>1.50</b>	<b>1.64</b>	<b>1.76</b>	<b>1.81</b>
Methods	Sittingdown								Smoking							
	Short-term motion prediction				Long-term motion prediction				Short-term motion prediction				Long-term motion prediction			
	80ms	160ms	320ms	400ms	560ms	640ms	720ms	1000ms	80ms	160ms	320ms	400ms	560ms	640ms	720ms	1000ms
ERD [18]	0.35	0.99	1.67	1.80	1.89	1.97	2.13	2.18	0.49	0.47	1.05	1.18	1.32	1.49	1.51	1.56
LSTM-3LR [18]	0.34	0.95	1.42	1.75	1.82	1.96	2.07	2.14	0.42	0.45	0.94	1.12	1.20	1.31	1.35	1.48
Res-GRU [1]	0.34	0.97	1.52	1.68	1.79	1.92	2.01	2.05	0.36	0.39	1.06	1.13	1.19	1.22	1.29	1.32
MHU [20]	0.34	<b>0.69</b>	1.38	1.53	1.66	<b>1.72</b>	<b>1.78</b>	1.93	0.35	0.42	0.96	1.08	1.12	1.17	1.24	1.30
SC-RNN	<b>0.34</b>	0.72	<b>1.37</b>	<b>1.51</b>	<b>1.65</b>	1.75	1.81	<b>1.92</b>	<b>0.35</b>	<b>0.41</b>	<b>0.94</b>	<b>1.06</b>	<b>1.10</b>	<b>1.15</b>	<b>1.21</b>	<b>1.28</b>
Methods	Takingphoto								Waiting							
	Short-term motion prediction				Long-term motion prediction				Short-term motion prediction				Long-term motion prediction			
	80ms	160ms	320ms	400ms	560ms	640ms	720ms	1000ms	80ms	160ms	320ms	400ms	560ms	640ms	720ms	1000ms
ERD [18]	0.71	0.78	1.02	1.20	1.27	1.46	1.49	1.53	0.38	0.69	1.14	1.43	1.56	1.62	1.70	1.79
LSTM-3LR [18]	0.74	0.64	0.91	1.19	1.29	1.40	1.45	1.51	0.35	0.65	1.13	1.41	1.52	1.60	1.68	1.77
Res-GRU [1]	0.31	0.56	0.87	1.04	1.18	1.25	1.19	1.37	0.36	0.62	1.15	1.40	1.47	1.58	1.69	1.72
MHU [20]	0.29	0.57	0.84	0.98	1.02	1.08	1.16	1.34	0.32	0.56	1.12	1.28	1.36	1.49	1.57	1.68
SC-RNN	<b>0.25</b>	<b>0.53</b>	<b>0.81</b>	<b>0.90</b>	<b>0.97</b>	<b>1.02</b>	<b>1.12</b>	<b>1.27</b>	<b>0.30</b>	<b>0.54</b>	<b>1.11</b>	<b>1.23</b>	<b>1.31</b>	<b>1.40</b>	<b>1.52</b>	<b>1.63</b>
Methods	Walking								Walkingtogether							
	Short-term motion prediction				Long-term motion prediction				Short-term motion prediction				Long-term motion prediction			
	80ms	160ms	320ms	400ms	560ms	640ms	720ms	1000ms	80ms	160ms	320ms	400ms	560ms	640ms	720ms	1000ms
ERD [18]	0.32	0.56	1.01	1.15	1.21	1.28	1.36	1.43	0.43	0.67	0.78	0.89	1.27	1.34	1.42	1.56
LSTM-3LR [18]	0.35	0.56	0.89	1.07	1.19	1.27	1.33	1.37	0.42	0.67	0.89	0.91	1.19	1.29	1.34	1.42
Res-GRU [1]	0.30	0.48	0.70	0.76	0.93	0.96	1.02	1.07	0.40	0.63	0.88	0.97	1.12	1.24	1.29	1.35
MHU [20]	0.34	0.54	0.69	0.78	0.89	0.98	1.07	1.12	0.41	0.55	0.61	0.79	0.97	1.08	1.16	1.27
SC-RNN	<b>0.32</b>	<b>0.47</b>	<b>0.54</b>	<b>0.63</b>	<b>0.72</b>	<b>0.78</b>	<b>0.83</b>	<b>0.88</b>	<b>0.41</b>	<b>0.43</b>	<b>0.50</b>	<b>0.58</b>	<b>0.67</b>	<b>0.73</b>	<b>0.89</b>	<b>1.02</b>

Encoder-Recurrent-Decoder (ERD) [18], 3-Layer Long Short-Term Memory cells (LSTM-3LR) [18], Residual Gated Recurrent Unit (Res-GRU) [1], and Modified Highway Unit (MHU) [20]. Table 3 shows the MAEs achieved by different methods on the H3.6M dataset. If can be seen that SC-RNN performs better than the alternatives, especially ERD and LSTM-3LR. In particular, SC-RNN has gained about 0.8 reduction compared with the MHU in terms of the long-term (1000ms) human motion prediction. This illustrates that SC-RNN is more effective than the other methods for predicting the future motion based on the observed human motion sequence.

We also compare the MAEs obtained by different meth-

ods on each human action in the H3.6M dataset, as shown in Table 2. SC-RNN achieves lowest MAE on most of the human actions. We can see that: 1) for the “eating” action, all the methods achieves satisfactory performance; 2) for the “posing” action, the MAEs on the long-term (1000ms) achieved by all methods are larger than 2.5, since the motions of different persons are largely diverse from each other; 3) for the “greeting” action, the proposed SC-RNN makes significant improvement than the other methods, since SC-RNN explores the spatial coherence among joints, which is crucial for modeling the human motion with large variation of the arm and leg motions. Although SC-RNN does not achieve the lowest MAE on the “posing” action, it

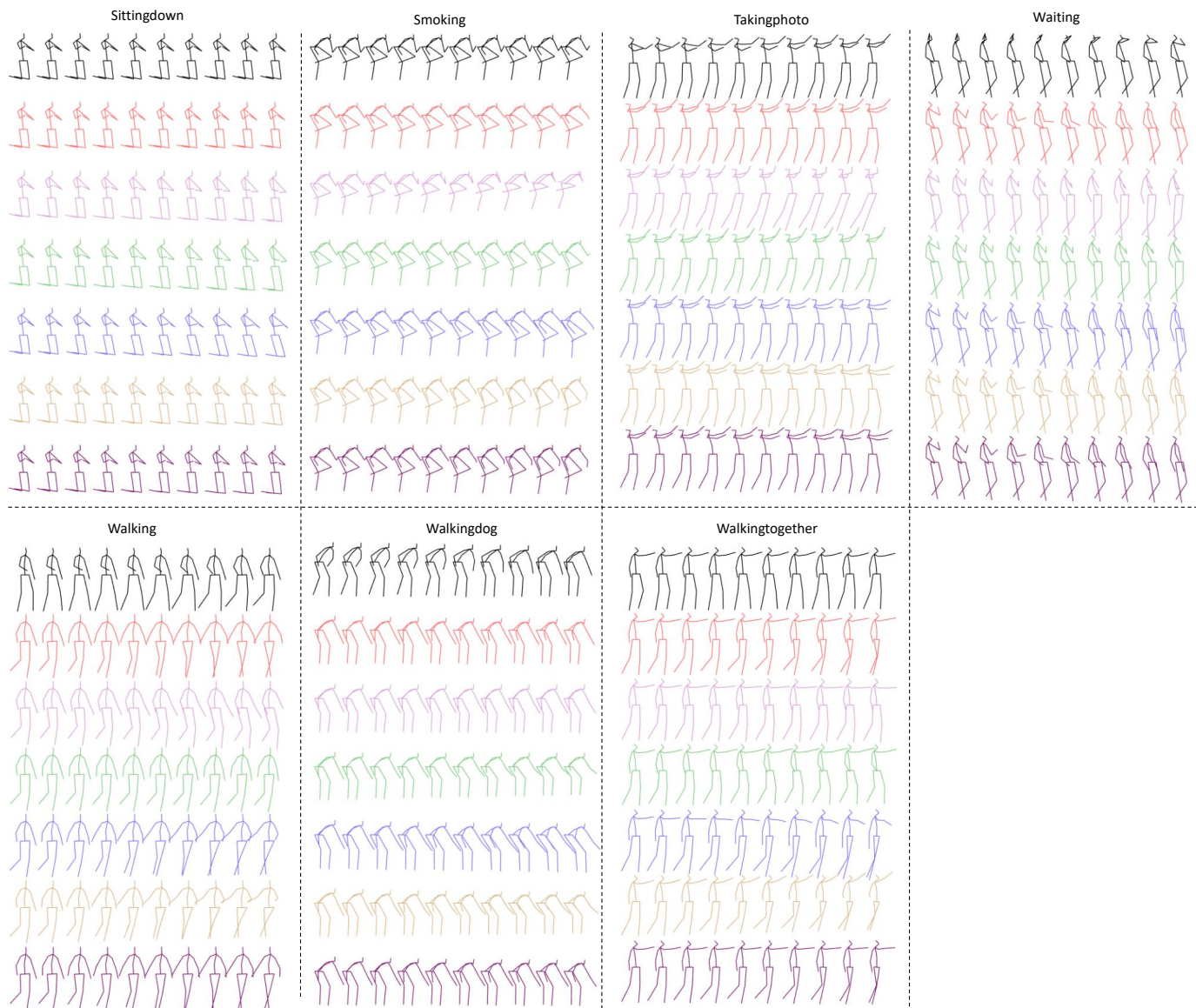


Fig. 6. Some visualized results of the motion prediction for all 15 actions. In each group, the first and the second rows are the observed motion and the ground-truth human motions, respectively; and the 3rd-7th rows are the human motion predicted by ERD [18], LSTM-3LR [18], Res-GRU [1], MHU [20] and the proposed SC-RNN, respectively. For better view, please see  $\times 3$  original color PDF. This figure follows Figure 5.

is comparable to the state-of-the-art method (MHU).

We also qualitatively compare the proposed SC-RNN with the state-of-the-art methods, as shown in Figure 5. SC-RNN generates the authentic motions for these actions, most of which are pretty closely to the ground-truth motions. For the human motions generated by ERD, LSTM-3LR, and Res-GRU, some details are not accurate compared with the ground truth, such as leg joints in the “eating” action. Since MHU considers all observed motions as motion context to predict the human motion, it can generate more reliable motions than ERD and LSTM-3LR. SC-RNN can predict motions with high accuracy in some details. For example, in the “greeting” action, the locations of two hands predicted by SC-RNN are more accurate than MHU in the long-term (1000ms) motion prediction.

## 5 CONCLUSIONS

In this work, for human motion prediction, we propose a novel Skeleton-joint Co-attention Recurrent Neural Networks (SC-RNN) to simultaneously capture the spatial coherence among joints and the temporal evolution among skeletons on a co-attention feature map, by utilizing all useful historical motion information as the motion context. The architecture of the proposed SC-RNN has three advantages. First, a new Skeleton-joint Co-Attention (SCA) is designed to dynamically learn a co-attention feature map on the skeleton-joint feature map of all the observed motions over time, which can refine the useful observed motion information by the different skeleton-joint attention factors. Second, a Skeleton-joint Co-attention GRU (SC-GRU) embedded with SCA is proposed to model human-joint motions and human-skeleton motions simultaneously in

spatiotemporal space. Third, a new weighted gram-matrix loss is presented to train the SC-GRU model in spatiotemporal space. Experimental results on human motion prediction well demonstrate that the proposed SC-RNN outperforms the related methods.

## REFERENCES

- [1] J. Martinez, M. J. Black, and J. Romero, "On human motion prediction using recurrent neural networks," in *IEEE Conference on Computer Vision and Pattern Recognition (CVPR)*, 2017.
- [2] J. Bütetage, M. J. Black, D. Kragic, and H. Kjellström, "Deep representation learning for human motion prediction and classification," in *IEEE Conference on Computer Vision and Pattern Recognition (CVPR)*, 2017.
- [3] A. M. Lehrmann, P. V. Gehler, and S. Nowozin, "Efficient non-linear markov models for human motion," in *IEEE Conference on Computer Vision and Pattern Recognition (CVPR)*, 2014.
- [4] L. L. Presti and M. La Cascia, "3d skeleton-based human action classification: A survey," *Pattern Recognition*, vol. 53, pp. 130–147, 2016.
- [5] W. Zhu, C. Lan, J. Xing, W. Zeng, Y. Li, L. Shen, and X. Xie, "Co-occurrence feature learning for skeleton based action recognition using regularized deep lstm networks," *arXiv*, 2016.
- [6] Y. Du, W. Wang, and L. Wang, "Hierarchical recurrent neural network for skeleton based action recognition," in *IEEE Conference on Computer Vision and Pattern Recognition (CVPR)*, 2015.
- [7] R. Vemulapalli, F. Arrate, and R. Chellappa, "Human action recognition by representing 3d skeletons as points in a lie group," in *IEEE conference on Computer Vision and Pattern Recognition (CVPR)*, 2014.
- [8] B. Mahasseni and S. Todorovic, "Regularizing long short term memory with 3d human-skeleton sequences for action recognition," in *IEEE Conference on Computer Vision and Pattern Recognition (CVPR)*, 2016.
- [9] R. Urtaşun, D. J. Fleet, and N. D. Lawrence, "Modeling human locomotion with topologically constrained latent variable models," in *Human Motion—Understanding, Modeling, Capture and Animation*, 2007, pp. 104–118.
- [10] V. Pavlovic, J. M. Rehg, and J. MacCormick, "Learning switching linear models of human motion," in *Advances in Neural Information Processing Systems (NeurIPS)*, 2001.
- [11] G. W. Taylor, G. E. Hinton, and S. T. Roweis, "Modeling human motion using binary latent variables," in *Advances in Neural Information Processing Systems (NeurIPS)*, 2007.
- [12] H. Yu, J. Wang, Z. Huang, Y. Yang, and W. Xu, "Video paragraph captioning using hierarchical recurrent neural networks," in *IEEE Conference on Computer Vision and Pattern Recognition (CVPR)*, 2016.
- [13] J. Chung, C. Gulcehre, K. Cho, and Y. Bengio, "Empirical evaluation of gated recurrent neural networks on sequence modeling," *arXiv preprint arXiv:1412.3555*, 2014.
- [14] S. Hochreiter and J. Schmidhuber, "Long short-term memory," *Neural computation*, vol. 9, no. 8, pp. 1735–1780, 1997.
- [15] X. Shu, J. Tang, G.-J. Qi, W. Liu, and J. Yang, "Hierarchical long short-term concurrent memory for human interaction recognition," *arXiv*, 2018.
- [16] X. Shu, J. Tang, G.-J. Qi, Y. Song, Z. Li, and L. Zhang, "Concurrence-aware long short-term sub-memories for person-person action recognition," in *IEEE Conference on Computer Vision and Pattern Recognition (CVPR) Workshops*, 2017.
- [17] R. Yan, J. Tang, X. Shu, Z. Li, and Q. Tian, "Participation-contributed temporal dynamic model for group activity recognition," in *ACM International Conference on Multimedia (ACM MM)*, 2018.
- [18] K. Fragkiadaki, S. Levine, P. Felsen, and J. Malik, "Recurrent network models for human dynamics," in *IEEE International Conference on Computer Vision (CVPR)*, 2015.
- [19] A. Jain, A. R. Zamir, S. Savarese, and A. Saxena, "Structural-mn: Deep learning on spatio-temporal graphs," in *IEEE Conference on Computer Vision and Pattern Recognition (CVPR)*, 2016.
- [20] Y. Tang, L. Ma, W. Liu, and W. Zheng, "Long-term human motion prediction by modeling motion context and enhancing motion dynamic," in *International Joint Conferences on Artificial Intelligence (IJCAI)*, 2018.
- [21] H. Wang and L. Wang, "Modeling temporal dynamics and spatial configurations of actions using two-stream recurrent neural networks," in *IEEE Conference on Computer Vision and Pattern Recognition (CVPR)*, 2017.
- [22] J. Liu, A. Shahroudy, D. Xu, A. C. Kot, and G. Wang, "Skeleton-based action recognition using spatio-temporal lstm network with trust gates," *IEEE Transactions on Pattern Analysis and Machine Intelligence*, vol. 40, no. 12, pp. 3007–3021, 2018.
- [23] R. Poppe, "A survey on vision-based human action recognition," *Image and vision computing*, vol. 28, no. 6, pp. 976–990, 2010.
- [24] G. Cheng, Y. Wan, A. N. Saudagar, K. Namuduri, and B. P. Buckles, "Advances in human action recognition: a survey," *arXiv*, 2015.
- [25] S. Herath, M. Harandi, and F. Porikli, "Going deeper into action recognition: A survey," *arXiv*, 2016.
- [26] V. Veeriah, N. Zhuang, and G.-J. Qi, "Differential recurrent neural networks for action recognition," in *IEEE International Conference on Computer Vision (ICCV)*, 2015.
- [27] S. Song, C. Lan, J. Xing, W. Zeng, and J. Liu, "An end-to-end spatio-temporal attention model for human action recognition from skeleton data," in *AAAI Conference on Artificial Intelligence (AAAI)*, 2017.
- [28] Y. Zhang, X. Liu, M.-C. Chang, W. Ge, and T. Chen, "Spatio-temporal phrases for activity recognition," in *European Conference on Computer Vision (ECCV)*, 2012.
- [29] K. Simonyan and A. Zisserman, "Two-stream convolutional networks for action recognition in videos," in *Neural Information Processing Systems (NeurIPS)*, 2014.
- [30] Y. Ke, R. Sukthankar, and M. Hebert, "Spatio-temporal shape and flow correlation for action recognition," in *IEEE Conference on Computer Vision and Pattern Recognition (CVPR)*, 2007.
- [31] C. Feichtenhofer, A. Pinz, and A. Zisserman, "Convolutional two-stream network fusion for video action recognition," in *IEEE Conference on Computer Vision and Pattern Recognition (CVPR)*, 2016.
- [32] G. Varol, I. Laptev, and C. Schmid, "Long-term temporal convolutions for action recognition," *IEEE Transactions on Pattern Analysis and Machine Intelligence*, vol. 40, no. 6, pp. 1510–1517, 2018.
- [33] J. Liu, A. Shahroudy, D. Xu, and G. Wang, "Spatio-temporal lstm with trust gates for 3d human action recognition," in *European Conference on Computer Vision (ECCV)*, 2016.
- [34] J. Wang, Z. Liu, Y. Wu, and J. Yuan, "Learning actionlet ensemble for 3d human action recognition," *IEEE Transactions on Pattern Analysis and Machine Intelligence*, vol. 36, no. 5, pp. 914–927, 2014.
- [35] P. Zhang, C. Lan, J. Xing, W. Zeng, J. Xue, N. Zheng *et al.*, "View adaptive recurrent neural networks for high performance human action recognition from skeleton data," *arXiv*, 2017.
- [36] H. Rahmani and M. Bennamoun, "Learning action recognition model from depth and skeleton videos," in *IEEE International Conference on Computer Vision (ICCV)*, 2017.
- [37] S. Yan, Y. Xiong, and D. Lin, "Spatial temporal graph convolutional networks for skeleton-based action recognition," *arXiv*, 2018.
- [38] Y. Yacoob and M. J. Black, "Parameterized modeling and recognition of activities," *Computer Vision and Image Understanding*, vol. 73, no. 2, pp. 232–247.
- [39] H. Rahmani and A. Mian, "Learning a non-linear knowledge transfer model for cross-view action recognition," in *IEEE Conference on Computer Vision and Pattern Recognition (CVPR)*, 2015.
- [40] I. Lillo, A. Soto, and J. Carlos Nieves, "Discriminative hierarchical modeling of spatio-temporally composable human activities," in *IEEE Conference on Computer Vision and Pattern Recognition (CVPR)*, 2014.
- [41] A. Shahroudy, T.-T. Ng, Q. Yang, and G. Wang, "Multimodal multipart learning for action recognition in depth videos," *IEEE Transactions on Pattern Analysis and Machine Intelligence*, vol. 38, no. 10, pp. 2123–2129, 2016.
- [42] J. Weng, C. Weng, and J. Yuan, "Spatio-temporal naive-bayes nearest-neighbor (st-nbnn) for skeleton-based action recognition," in *IEEE Conference on Computer Vision and Pattern Recognition (CVPR)*, 2017.
- [43] Y. Hou, Z. Li, P. Wang, and W. Li, "Skeleton optical spectra-based action recognition using convolutional neural networks," *IEEE Transactions on Circuits and Systems for Video Technology*, vol. 28, no. 3, pp. 807–811, 2018.
- [44] Z. Huang, C. Wan, T. Probst, and L. Van Gool, "Deep learning on lie groups for skeleton-based action recognition," in *IEEE Conference on Computer Vision and Pattern Recognition (CVPR)*, 2017.
- [45] A. Shahroudy, T.-T. Ng, Y. Gong, and G. Wang, "Deep multimodal feature analysis for action recognition in rgb+ d videos," *IEEE*

- Transactions on Pattern Analysis and Machine Intelligence*, vol. 40, no. 5, pp. 1045–1058, 2018.
- [46] I. Sutskever, J. Martens, and G. E. Hinton, “Generating text with recurrent neural networks,” in *International Conference on Machine Learning (ICML)*, 2011.
- [47] Z. Shi and T.-K. Kim, “Learning and refining of privileged information-based rnns for action recognition from depth sequences,” in *IEEE Conference on Computer Vision and Pattern Recognition (CVPR)*, 2017.
- [48] J. Liu, G. Wang, P. Hu, L.-Y. Duan, and A. C. Kot, “Global context-aware attention lstm networks for 3d action recognition,” in *IEEE Conference on Computer Vision and Pattern Recognition (CVPR)*, 2017.
- [49] J. K. Aggarwal and Q. Cai, “Human motion analysis: A review,” *Computer Vision and Image Understanding*, vol. 73, no. 3, pp. 428–440, 1999.
- [50] C. Ionescu, D. Papava, V. Olaru, and C. Sminchisescu, “Human3.6m: Large scale datasets and predictive methods for 3d human sensing in natural environments,” *IEEE Transactions on Pattern Analysis and Machine Intelligence*, vol. 36, no. 7, pp. 1325–1339, 2014.
- [51] J. M. Wang, D. J. Fleet, and A. Hertzmann, “Gaussian process dynamical models for human motion,” *IEEE Transactions on Pattern Analysis and Machine Intelligence*, vol. 30, no. 2, pp. 283–298, 2008.
- [52] D. Pavlo, D. Grangier, and M. Auli, “Quaternet: A quaternion-based recurrent model for human motion,” *British Machine Vision Conference (BMVC)*, 2018.
- [53] V. Ramanathan, J. Huang, S. Abu-El-Haija, A. Gorban, K. Murphy, and L. Fei-Fei, “Detecting events and key actors in multi-person videos,” in *IEEE Conference on Computer Vision and Pattern Recognition (CVPR)*, 2016.
- [54] C. Cao, C. Lan, Y. Zhang, W. Zeng, H. Lu, and Y. Zhang, “Skeleton-based action recognition with gated convolutional neural networks,” *IEEE Transactions on Circuits and Systems for Video Technology*, 2018.